MitoQ Promotes M2-Like Macrophage/Microglia Polarization And Attenuates Apoptosis After Spinal Cord Injury Through Mitochondria-Dependent Pathway

Tengli Huang
Shanghai Jiaotong University Affiliated Sixth People's Hospital
Junqing Lin
Shanghai Jiaotong University Affiliated Sixth People's Hospital
Junjie Shen
Shanghai Jiaotong University Affiliated Sixth People's Hospital
Xianyou Zheng (zhengxianyou@126.com)
Shanghai Jiaotong University Affiliated Sixth People's Hospital

Research

Keywords: Spinal cord injury, macrophage/microglia, neuroinflammation, apoptosis, mitochondria, mitochondrial dysfunction, MitoQ, ROS, oxidative stress, DCFH-DA, 2,7-Dichlorodi -hydrofluorescein diacetate

Posted Date: June 29th, 2021

DOI: https://doi.org/10.21203/rs.3.rs-643266/v1

Abstract

Background: Mitochondrial dysfunction and macrophage/microglia mediating inflammation are critical pathological process components of secondary injury in spinal cord injury (SCI), which lead to impaired regeneration and function recovery. Mitochondria is essential to macrophage/microglia metabolism and polarization. However, there are few research in SCI on mitochondrial dysfunction and macrophage/microglia polarization modulation by MitoQ, a mitochondrial-specific antioxidant. Therefore, we tried to investigate whether MitoQ could promote function recovery after SCI and its potential mechanism.

Methods: A T10 spinal cord clip compression model was established in female C57BL/6 mice. MitoQ (1 mg/ml) was injected intraperitoneally on day 0, 1, 2 after SCI. Immunofluorescence assay (iNOS/Arg-1) was performed on day 3 and 14 to evaluate macrophage/microglia polarization after SCI. Basso Mouse Scale (BMS) score and footprint analysis were used to evaluate function recovery. Haematoxylin-eosin (HE) and Luxol Fast Blue (LFB) staining were used to evaluate tissue preservation and myeline loss. Western-blotting (mfn-1/2/drp-1), flow cytometry, immunofluorescence assay (iNOS/Arg-1) and fluorescence assay (Mitosox Red/ DCFH-DA) were used to evaluate in-vitro mitochondrial function and macrophage/microglia polarization. Tunel staining, Hochest staining and Western-blotting (Bax/Bcl-2/Cleaved-caspase-3) were used to evaluate cell apoptosis in BV2 cells and established SCI animal models.

Results: Compared with SCI group, MitoQ group showed reduced M1-like polarization with enhanced M2-like polarization on day 3 and day 14 after SCI. MitoQ group promoted function recovery and tissue preservation on day 28. MitoQ attenuated mitochondrial biodynamic imbalance and reduced mitochondrial-specific reactive oxygen species (ROS) production in BV2 cells. MitoQ inhibited cell apoptosis resulting from in-vitro LPS challenging and in-vivo SCI.

Conclusion: MitoQ improves function recovery and tissue preservation after SCI through the promotion of M2-like polarization of macrophage/microglia, inhibition of cell apoptosis and following neuroinflammation with the improvement of mitochondrial function and decreasing oxidative stress. Taken together, our results suggest that mitochondrial function modulation is a potential treatment option of post-SCI macrophage/microglia polarization dysfunction, following neuroinflammation and function impairment.

Background

Spinal cord injury (SCI), the major contributor of partial or complete sensor-motor disability which brings enormous economic burden to society, remains a challenging clinical problem. In general, SCI is divided into primary and secondary injury. Despite primary injury (mostly mechanical injury), secondary injury includes hemorrhage, mitochondrial dysfunction, oxidative stress, neuron death, prolonged neuroinflammation, axonal demyelination and degeneration etc[1]. Prolonged neuroinflammation, mainly

mediated by macrophage/microglia, is one of the major causes of unsatisfied neuro-regeneration after SCI resulting from continuous pro-inflammatory factors releasing and microenvironment disruption.

Microglia, commonly considered as resident macrophage in central nervous system (CNS)[2], is vital immune cell that mediates cell proliferation, scar formation and myeline remodeling following SCI[3]. Microglia is highly flexible as macrophage and it can be activated and shifted into different phenotypes, which can be generally divided into M1-like and M2-like subtypes in response to various stimuli in different pathological periods. M1-like microglia, commonly stimulated by TNF-α and IFN-γ, is defined to be neurotoxic mainly through secretion of pro-inflammatory cytokines: TNF-α, IL-6 and IL-1β, disturbance of microenvironment and contribution to scar formation[4]. While M2-like microglia is considered as neuroprotector for its essential role in tissue repair and anti-inflammatory cytokines secretions[5]. Therefore, macrophage/microglia polarization, the key contributor of post-SCI microenvironment formation, has been proved to be vital to SCI treatment[6,7].Given that, research of macrophage/microglia phenotypes modulation have become a hot point recently[8–10].

Macrophage/microglia metabolism including glucose, fatty acid and amino acid has been found to be essential to macrophage activation and polarization[11]. Given the importance of metabolism in macrophage regulation, mitochondria, the major energy factory of cells, shows enormous potential in macrophage regulation. SCI-leading mitochondrial dysfunction is a common pathological process in secondary injury which resulting in oxidative stress and cell apoptosis/death. Recently, mitochondrial function has been found to be essential to macrophage polarization[11]. However, there are few research have been done to investigate the relationship between mitochondrial dysfunction and macrophage/microglia polarization dysfunction in SCI. Mitoquinone (MitoQ) is a mitochondrial-targeted antioxidant protecting treated mitochondria from oxidative stress/reactive oxygen species'(ROS) damage to mitochondrial proteins and DNA[12]. MitoQ plays a neuroprotective role in neurologic disease[13]. It's beneficial to the recovery of intracerebral hemorrhage[14] and neurological pain[15]. The potential role of MitoQ in SCI neuroprotection and underlying mechanism requires further research to discover.

Therefore, in this study we try to investigate MitoQ's role in modification of neuroinflammation and macrophage/microglia polarization phenotypes and whether it can be beneficial to post-SCI function recovery and tissue preservation.

Methods

Cell culture

BV2 murine cells used in this experiment were purchased from Shanghai Cell Research Center (Shanghai, China). Cells were maintained in DMEM high glucose medium containing 10% fetal bovine serum (Gibico, USA) and 1% penicillin/streptomycin (Invitrogen, USA). Humidified incubator containing 5% CO2 at 37 ℃ was used to keep cells. After reaching about 80% in culturing plates, cells were considered to be suitable for following experiments.

Cell treatment

Prior to Lipopolysaccharide (LPS) challenging, cells in MitoQ group were pretreated with MitoQ (200 nM, MCE, USA) for 12 h. Then cells in LPS group were treated with 100 ng/ml LPS (Aladdin, China) for 24 and 48 h, and cells in MitoQ group were treated with the mixture of LPS (100 ng/ml) and MitoQ (200 nM).

Animals

Female C57BL/6 mice aged from 10 to 14 weeks old were purchased from Laboratory Animal Center of Shanghai Jiao Tong University. Animals were housed in facility which controlled its humidity at 55-65% and temperature at 24 ± 3 ℃ with 12hr period of light/dark cycle. Food and water were provided and animals had free access to the supply. All procedures were approved by the Institutional Animal Care and Use Committee (IACUC) of Shanghai Jiao Tong University affiliated Sixth People's Hospital, China. All study methods were in accordance with China's regulations on experimental animal usage, which were consistent with Animal Research: Reporting of In Vivo Experiments (ARRIVE) guidelines.

SCI model establishment

The establishment of SCI clip-compression model was based on the research reported previously[16]. After animals were anesthetizing with intraperitoneally injection of ketamine (50 mg/kg) and xylazine (3 mg/kg), skin preparation was performed prior to surgery. A 1 cm incision was made after identifying thoracic spine at level 10, then surrounding skin and tissue were manually removed using ophthalmic scissors. After that, animals received a T10 laminectomy to expose the spinal cord. Animals in sham group only received the laminectomy. Next, a 30-g aneurysm clip was applied to the T10 level for 1 min to induce compression injury. Then the surgical site was closed by muscle, fascia and skin suturing. In MitoQ groups, MitoQ (1 mg/ml) was injected intraperitoneally immediately after SCI and on day 1, 2, respectively. After fully recovery on the heating pad (37 ℃), animals were housed and received manual bladder expression twice per day until a primary bladder reflex was re-established. Antibiotics and analgesic were used as routine on day 0, 1, 2, 3 to prevent infection and excessive pain.

Mitosox Red staining

For mitochondrial specific superoxide radical generation measurement, MitoSOX™ Red Mitochondrial Superoxide Indicator (M36008, Invitrogen, USA) was used according to manufacturer's instruction. In brief, cells were plated and cultured in 24-well (for fluorescence assay) or 6-well (for flow cytometry) plates. After receiving treatment as described previously, cells were washed for 3 times with Hank's solution (37 ℃) after removing culturing medium. Then cells were incubated with Mitosox Red (5 um) and Hoechst staining (5 ug/ml, Beyotime, China) for 30 min in light-proof humidified chamber at 37 °C. Then cells were ready for following experiments.

Cellular ROS assay

Generation of cellular ROS was assessed by DCFH-DA probe (Reactive Oxygen Species Assay Kit, Beyotime, China). All procedures were applied according to manufacturer's introduction. In brief, cells were plated and cultured in 24-well (for fluorescence assay) or 6-well (for flow cytometry) plates. After receiving treatment as described previously, cells were washed 3 times with Hank's solution (37 ℃) after removing medium. Then DCFH-DA (10 uM) was added to each well following by 20-miniute incubation in light-proof humidified chamber at 37 °C. Then cells were ready for following experiments.

Flow cytometry

For Mitosox red and DCFH-DA assay, cells were plated and cultured in 6-well plates, then received treatment as described previously. For macrophage/microglia polarization assay, cells were plated and cultured in 6-well plates. After harvesting, cells were washed with PBS and stained with anti-iNOS/Arg-1 antibody (17-5920-80/12-3697-82, eBioscience, USA). Flow cytometry was performed using a BD FACS Aria (BD Bioscience, USA). And data was analyzed using FlowJo Software (Tree Star Inc, USA).

Western blotting

For the determination of protein expression, Western-blotting analysis was performed. BV2 cells cultured in six-well plates were treated as described previously. Firstly, cells were rinsed with pre-cold PBS for 3 times and then lysed with RIPA-Buffer (Beyotime, China) and protease inhibitor cocktail (Beyotime, China) on ice for 30 min. Then lysed extraction were centrifugated for 10 min, 12000g at 4 °C. BCA protein assay kit (Beyotime, China) was used to determine protein content in all samples. SDS-polyacrylamide gel electrophoresis was performed followed by transferring to polyvinylidene fluoride (PVDF) membranes for 70 min at 250 mA. Then transferred PVDF membranes were blocked with 5% fat-free milk dissolved in TBST. Membranes were incubated with primary antibody overnight at 4 °C. On the next day, appropriate HRP-conjugated secondary antibody (1:5000) was added for one-hour incubation at room temperature. After several times of washing with TBST, bands were scanned and analyzed after adding enhanced chemiluminescence (ECL, Millipore, USA) through imaging system. Bands were normalized to β-actin. And data were analyzed and presented through ImageJ and GraphPad Prism version 9 (GraphPad Software, USA).

The antibodies used in this research included: Mfn-1/2(1:1000, ab57602, Abcam, UK), Drp-1 (1:1000, ab184247, Abcam, UK), B cell lymphoma (Bcl)-2 (1:1000, 3498S, Cell Signaling Technology, USA), Bcl-2-associated X factor (Bax) (1:1000, 14796S, Cell Signaling Technology, USA), cleaved-caspase-3 (1:1000, 9664S, Cell Signaling Technology, USA), β-actin (1:1000, 4970S, Cell Signaling Technology, USA).

Immunofluorescence staining

After receiving prior treatment, cells and tissue slides were applied with 30-miniute 4% paraformaldehyde fixation at room temperature following by PBS washing for 3 times and 15-miniute 0.5% Triton X-100 permeabilization. Then cells and slides were incubated with 5% donkey serum for 1 h at room temperature. After incubation with primary antibody overnight at 4 °C, cells and slides were washed for 3

times by PBS and incubated with appropriate secondary antibodies for 1 h. Then incubated cells and slides were treated with DAPI staining medium (Beyotime, China) for 10 min at 37 ℃. Images were captured by fluorescence microscope (DMI8, Leica, Germany)

The primary antibodies used in this research included: iNOS (1:100, ab15323, Abcam, UK), Arg-1 (1:100, ab91279, Abcam, UK).

Histological staining

Hematoxylin and Eosin (HE) staining and Luxol-fast-blue (LFB) staining were performed to evaluate the tissue preservation and myeline loss on day 28 after SCI at the transection of lesion center. The protocol of HE and LFB staining was based on the well-established protocol reported previously[17,18]. Pictures were captured with DMI6 microscopy (Leica, Germany).

Function analysis

To evaluate function recovery of animals in SCI after MitoQ treatment, BMS test and footprint analysis were performed. BMS was used to evaluate the motor function recovery of the hind limbs. In brief, two independent researchers were trained and blind to the grouping of tested animals. BMS test were performed on the day before the surgery, day 0, 7, 14, 21 and 28.

Footprint analysis was performed through a CatWalk gait analysis system as reported previously[19]. Animals were pre-trained before the examinations. On day 28 after SCI, animals received the gait examinations at least three times per round. Pictures and videos were captured through camera of the system.

Statistical analysis

All statistical analysis were performed through GraphPad Prism version 9. And all experiments were repeated at least three times. Data are expressed in the form of mean ± standard error of the mean from three independent examinations. Student's t test when performed to examine the statistical significance between two groups. One-way analysis of variance (ANOVA) with Bonferroni tests analysis was conducted to examine the differences among three groups. A p value lower than 0.05 was considered to be statistically significant.

Results

Macrophage/microglia polarization dysfunction after SCI

Activation of macrophage/microglia is a vital pathological process in SCI, which is the major contributor of microenvironment disturbance after SCI. And in the acute period, M1-like macrophage/microglia are in the majority and remains predominant (Figure. 1A, C, p□0.0001) and the expression of M2-like macrophage/microglia is transient and significantly lower than M1-like subtypes (Figure. 1B, D, p□

0.0001). And in subacute phase, the expression of M1-like macrophage/microglia is still significantly higher than that in Sham group (Figure. 2A, C, p□0.001). However, the expression of M2-like macrophage/microglia decreased and showed no significant difference comparing to that in Sham group (Figure. 2B, D). As previously reported, macrophage polarization in the late phase of organ injury repair is commonly transferred into an anti-inflammatory subtypes[20] (commonly considered as M2-like subtypes). The previous results showed that macrophage/microglia polarization dysfunction (prolonged M1 subtypes and transient M2 subtypes) leaded to a prolonged neuroinflammation and might be one of the major causes of impaired recovery of SCI.

MitoQ attenuates LPS-induced mitochondrial biodynamic imbalance in BV2 cells

To investigate MitoQ's potential role in macrophage/microglia function modulation, we firstly used LPS, a common M1-polarization-inducing factor, to induce M1-like polarization in BV2 cells. To identify whether mitochondrial biodynamic is disturbed in M1-like macrophage/microglia, the expression of mitochondrial biodynamic related protein (Mfn-1/2 and Drp-1) and their inner balance were measured through Western blotting assay (Figure. 3A). As shown in Figure. 3B, the protein expression of Mfn-1/2 of MitoQ and LPS group both decreased significantly comparing to Control group (n=3 , MitoQ vs Control: p□0.01, LPS vs Control: p□0.001) after 24-hour treatment of LPS. And the protein level of Drp-1 among three groups shows no significant change. And the ratio of Mfn-1/2 to Drp-1 of both groups showed significant decrease comparing to Control group (n=3, MitoQ vs Control: p□0.01, LPS vs Control: p□0.01), which indicated the disturbance of mitochondrial biodynamic balance and short-time MitoQ treatment failed to rescue the mitochondrial biodynamic imbalance. While after 48-hour treatment, the expression of Mfn-1/2 increased significantly in MitoQ group comparing to LPS groups (n=3, p□0.0001). And expression of Drp-1 decreased significantly in MitoQ group (n=3, p□0.01). The ratio of Mfn-1/2 to Drp-1 in MitoQ group increased significantly comparing to LPS group (n=3, p□0.0001). Given that, MitoQ took time to function and rescue the mitochondrial biodynamic imbalance through inhibition of mitochondrial fission and promotion of its fusion in-vitro.

MitoQ reduces LPS-induced ROS production and following oxidative stress in BV2 cells

Microenvironment oxidative stress is also an important secondary pathological process after SCI. Mitochondria, which is considered as the main source of cellular ROS in cells, is a potential target of ROS scavenger. To investigate MitoQ's effect on oxidative stress inhibition, the mitochondrial-specific ROS production was assayed through Mitosox Red staining with fluorescence assay and flow cytometry. In fluorescence assay, the integrated density ratio to control group of Mitosox Red in MitoQ group significantly decreased comparing to LPS group (Figure. 4A, B, p□0.0001). And the result of flow cytometry also verified this result (Figure. 4D). Same result was found in DCFH-DA, a cellular ROS staining (Figure. 4A, C, p□0.0001). These results indicated MitoQ could rescue mitochondrial function through inhibition of mitochondrial-derived oxidative stress and ROS production.

MitoQ attenuates LPS-induced and SCI-induced apoptosis through mitochondrial function improvement

Cell death, apoptosis following primary mechanical SCI are important pathogenesis process contributing to impaired tissue preservation and function recovery of spinal cord. And mitochondria is the key to apoptotic process. In-vitro examinations including Western blotting and Hochest staining were implemented. As shown in Figure. 5A, 24-hour LPS treatment could lead to BV2 cells apoptosis with significant increase of apoptosis-related protein (Bax and Cleaved-caspase-3) and significant decrease of anti-apoptotic protein (Bcl-2) expression comparing to Control group (Bax and Cleaved-caspase-3, n=3, Bax: p□0.05, Cleaved-caspase-3: p□0.001, Bcl-2: p□0.001). While MitoQ treatment successfully rescue the apoptosis caused by LPS challenging with the significant decrease of Bax and cleaved-caspase 3 expression and significant increase of Bcl-2 expression comparing to LPS group (Bax: p□0.0001, Cleaved-caspase 3: p□0.0001, Bcl-2: p□0.05), which indicated that MitoQ treatment could inhibit LPS-induced apoptosis in BV2 cells. Hochest staining was performed to verify the result of Western blotting. Nuclear condensation and fragment were observed in LPS group, while MitoQ succeeded in inhibition of these apoptotic process (Figure. 5B). These results indicated that MitoQ could inhibit apoptosis of macrophage/microglia under LPS challenging in-vitro.

In-vivo examination was performed to identify MitoQ' anti-apoptosis effect in SCI animal models (Figure. 6). To further confirm MitoQ's role in apoptosis inhibition, Tunel staining was performed on day 3 and day 14 after SCI. As performed in Figure. 5C-D, significant decrease in Tunel-positive area was found in MitoQ group comparing to SCI group (p□0.0001), which indicated that MitoQ could inhibit cell apoptosis in-vivo. Taking these results together, we found that MitoQ could inhibit cell apoptosis through promotion of mitochondrial function in-vitro and in-vivo.

MitoQ promotes function recovery, tissue sparing and neural preservation after SCI

To assess the effect of MitoQ on function recovery after SCI, two behavioral tests were implemented. BMS test was applied weekly among Sham, SCI and MitoQ groups after SCI. On day 7 after SCI, no significant change was found between the BMS score of SCI and MitoQ groups. On day 14, 21, 28, MitoQ group showed significant increase in BMS score comparing to SCI group (Figure. 7A, n=3, p□0.05). These data indicated that MitoQ might improve function recovery after the acute phase of SCI. And in footprint assay carried out through catwalk analyzer on day 28 after SCI, the footprint and hindlimb mean intensity were measured. (Figure. 7B). MitoQ groups showed clearer footprint of hindlimb comparing to SCI group (Figure. 7B-a, b) and the hindlimb intensity of MitoQ groups increased significantly (Figure. 7C, n=3, p□ 0.0001).

SCI could lead to tissue impairment and loss of myeline which influence nerval signal transmission and function recovery (Figure. 8A). HE staining indicated that MitoQ could significantly promote tissue sparing after SCI (Figure. 8B). Demyelinated area on day 28 was evaluated through LFB staining. And demyelinated area in MitoQ group was significantly smaller than that in SCI group (Figure. 8C). These findings indicated that MitoQ could promote tissue sparing and neural preservation after SCI.

Modulation of mitochondrial function regulates macrophage/microglia polarization after SCI

Macrophage/microglia polarization dysfunction is the key pathogenesis of secondary injury and the leading cause of prolonged neuroinflammation after SCI. To evaluate MitoQ's effect on the modulation of macrophage/microglia polarization, immunofluorescence staining was implemented. INOS-positive cells were considered as M1-like polarized cells and Arg-1-positive cells was considered as M2-like polarized cells (Figure. 9A, 10A). In acute phase of SCI (Day 3), MitoQ group could significantly decrease the expression of iNOS-positive cells and significantly increase the expression of Arg-1-positive cells comparing to SCI group, which indicated that MitoQ could modulate macrophage/microglia polarization towards M2-like subtypes after acute SCI (Figure 9B-C, p□0.0001, SCI group from Figure. 1A-B). And similar results were confirmed in day 14 examinations (Figure. 10B-C, p□0.0001, SCI group from Figure. 2A-B), which indicated that MitoQ could inhibit M1-like polarization of macrophage/microglia and promote M2-like polarization after SCI in the subacute phase. These data suggested that mitochondrial function modulation was a potential treatment target for post-SCI macrophage/microglia polarization dysfunction.

Modulation of mitochondrial function regulate macrophage/microglia polarization in BV2 cells

To verify MitoQ's effect in modulation of macrophage/microglia polarization, in-vitro experiments including immunofluorescence staining and flow cytometry were implemented. In accordance with the findings in SCI animal models, MitoQ could significantly decrease the expression of iNOS-positive cells in LPS-challenging BV2 cells after 48-hour-treatment comparing to Control and LPS groups (Figure 11A, C, p □0.0001). And MitoQ could significantly increase the expression of Arg-1-positive cells under equal conditions (Figure. 11B, D, p□0.0001). To further confirm this finding, flow cytometry (x-axis: iNOS; y-axis: Arg-1) was performed. Similar result confirmed that MitoQ could inhibit the M1-polarization after 24- and 48-hour-LPS challenging and partially promote M2-like polarization (Figure. 11E). These data confirmed what we found in the SCI models that MitoQ could modulate macrophage/microglia polarization through a mitochondrial-dependent pathway, which indicated that mitochondrial dysfunction might be the core of the macrophage polarization dysfunction and cellular apoptosis (Figure. 12).

Discussion

Increasing evidence have suggested the important role of mitochondria in the macrophage/microglia polarization modulation, but few related research have been performed in SCI. In the present study, we investigated the effect of MitoQ, a mitochondria-specific antioxidant, on SCI and its underlying mechanism through in-vitro and in-vivo examinations. These results indicate that MitoQ could promote M2-like polarization and inhibit M1-like polarization which attenuate neuroinflammation after SCI and promote tissue preservation and neural repair through the mitochondrial-dependent pathway. MitoQ could inhibit cell apoptosis after SCI and LPS challenging in BV2 cells which resulted in the improved locomotor function recovery and tissue preservation. These data suggested that mitochondrial function could be considered as a potential therapeutic target and MitoQ's reliable role in SCI treatment.

In SCI, prolonged neuroinflammation, a major contributor to poor self-regeneration and ongoing damage of spinal cord[21], has become an important treatment target. Recently, specific treatments including nafamostat mesilate[22], mulberrin[23], matrix metalloproteinase-8[24], zinc[25] have been used to reduce neuroinflammation in SCI and proved to be neuro-protective and contributive to locomotor recovery. Though prolonged and severe neuroinflammation has been considered to impair SCI self-regeneration and function recovery, mild neuroinflammation in SCI has been proved to be benefit to rehabilitative training result which indicates that controllable and mild inflammation can remove cell debris and dead cells to promotes recovery[26]. And microglia is considered as the crucial mediating cell in post-SCI neuroinflammation. The high flexibility of macrophage/microglia has been paid much attention in central nervous system injury. Macrophage/microglia can be shifted into different subtypes including M1-like type and M2-like type in response to distinct stimuli. M1-like macrophage/microglia is considered to be neurotoxic while M2-like type is neuroprotective[27]. Thus, modulation of macrophage/microglia polarization is an important treatment target in SCI.

In our study, we found that LPS-challenging M1-like BV2 cells showed significantly impaired mitochondrial function and biodynamic imbalance with decreasing ratio of Mfn-1/2 to Drp-1 and increasing production of cellular and mitochondrial specific ROS. Recent studies have revealed the important relationship between macrophage polarization and mitochondrial function. Yujia Yuan and colleagues found that mitochondrial ROS contributed to M1 macrophage polarization in diabetes[28]. Calcium uptake, an important physiological process of mitochondria, is essential to M2-like macrophage polarization[29]. Similar results were also found in skeletal muscle regeneration[30]. Given that, attenuation of mitochondrial damage/dysfunction has become a critical treatment target in macrophage phenotype modulation and following inflammation. IL-25, a member of IL-17 cytokine family, was found to regulate M2-like macrophage polarization and promote mitochondrial function[31]. Inhibition of AMP Kinase could enhance M1-like macrophage polarization and reduce mitochondrial biogenesis in chronic kidney disease[32]. Pyruvate dehydrogenase kinase 1 was found to take part in macrophage polarization through the regulation of glucose metabolism (partial function of mitochondria)[33]. And MitoQ is considered as a mitochondrial-targeting antioxidant, which can quickly protect mitochondria from oxidative stress. In in-vitro examinations, we found that MitoQ could rebalance the mitochondrial biodynamic imbalance, inhibit mitochondrial-specific and cellular ROS production which indicated MitoQ's role in mitochondrial function modulation. These results are consistent with former research. However, there are few research on the relationship between mitochondrial function modulation and macrophage/microglia polarization in SCI.

In this study, it's the first time to evaluate the association between mitochondrial dysfunction rescue with MitoQ and its modulation of macrophage/microglia polarization in SCI. As mentioned above, mitochondria function is vital to macrophage/microglia polarization modulation. Classification of microglia is similar to that in macrophage. Microglia can be classified into M1- like type and M2-like type. The polarization statement of microglia is vital to pathogenesis process of multiple diseases. And in neurological disorders like Parkinson's disease and Alzheimer's Disease, modulation of microglia

phenotypes is still the hot zone. Further cellular and molecular mechanisms were investigated in microglia modulation. Triggering receptor expressed on myeloid cells-2 (TREM2) was found to be essential to microglia polarization in Parkinson's disease that it could altering M1 microglia to M2 subtypes[34]. Ion channel including potassium channel/ Kir6.1-containing ATP-sensitive potassium is the modulation of microglia phenotypes[35]. As uncontrollable neuroinflammation impairs self-regeneration ability of spinal cord following SCI. Recently, macrophage metabolism, which contributing to immunometabolism, has become increasingly important and highlighted. Innate immunity can be characterized by metabolic reprogramming change. A recent review concluded 6 major metabolic pathways in macrophage subsets including amino acid, glycolysis, oxidative phosphorylation (OXPHOS), pentose phosphate pathway (PPP), fatty acid synthesis (FAS) and fatty acid oxidation(FAO)[11]. As mitochondria is a vital organelle participating in energy production, it takes part in multiple pathways among those six pathways. Inducible NO synthase (iNOS) and arginase-1(Arg-1) expression is typical marker of M1 and M2 macrophage. Arginine is coverted into nitric oxide(NO) through iNOS in M1 macrophage and it's metabolized by Arg-1 in M2 macrophage[36].While in energy production, M1-like macrophage is characterized by enhanced PPP and disrupted TCA cycle and M2-like macrophage is mainly dependent on glycolysis[37]. In accordance with the result of in-vitro study, MitoQ could inhibit M1-like polarization and promote M2-like polarization on day 3 and day 14 in established SCI animal model. Significant function recovery and tissue preservation were observed in MitoQ treatment group. These results indicate mitochondria is an important treatment target for prolonged neuroinflammation resulting from macrophage/microglia polarization dysfunction in SCI.

Cell apoptosis can be considered as the ultimate destiny of neuron and surrounding cells at severely injured site of SCI which leads to neural deficiency and tissue loss. Mitochondria is considered as the multifaceted regulators of cell death[38]. Thus, modulation of mitochondrial function can be beneficial to cell apoptosis after SCI. And our results showed that rescue of mitochondrial function through MitoQ treatment could significantly inhibit the apoptosis after SCI and LPS challenging.

Limitation of this research must be declared that the underlying molecular mechanism of how mitochondria modulate macrophage/microglia polarization hasn't been mentioned. As mitochondria is the vital regulator of cell metabolism and destiny, there are various pathway related to mitochondria modulation including mechanistic/mammalian target of rapamycin (mTOR) pathway[39,40] and NF-κB pathway[41,42]. Molecular mechanism of this process requires further research to shed light on the inner relationship.

Conclusion

MitoQ improves function recovery and tissue preservation after SCI through the promotion of M2-like polarization of macrophage/microglia and inhibition of cell apoptosis and following neuroinflammation. Taken together, our results suggest that mitochondrial modulation is a potential treatment target of post-SCI macrophage/microglia polarization dysfunction and neuroinflammation.

Abbreviations

SCI: Spinal cord injury; CNS: Central nervous system; MitoQ: Mitoquinone; TNF-α: tumor necrosis factor alpha; IFN-γ: Interferon-gamma; ROS: reactive oxygen species; IACUC: the Institutional Animal Care and Use Committee; HE: Hematoxylin and Eosin; TUNEL: Terminal

deoxynucleotidyl transferase-mediated deoxyuridine triphosphate nick end labeling; BMS: Basso Mouse Scale; OXPHOS: oxidative phosphorylation; PPP: pentose phosphate pathway; FAS: fatty acid synthesis; FAO: fatty acid oxidation; ARRIVE: Animal Research: Reporting of In Vivo Experiments; ECL: enhanced chemiluminescence; Bcl: B cell lymphoma; Bax: Bcl-2-associated X factor; DAPI: 4',6-diamidino-2-phenylindole

Declarations

Ethics approval and consent to participate: All procedures were approved by the Institutional Animal Care and Use Committee (IACUC) of Shanghai Jiao Tong University, China. All study methods were in accordance with China's regulations on experimental animal usage, which were consistent with Animal Research: Reporting of In Vivo Experiments (ARRIVE) guidelines.

Consent for publication: Not applicable.

Availability of data and materials: Not applicable.

Competing interests: The authors declare that they have no competing interests.

Funding: This work was supported by National Natural Science Foundation of China, 81974331.

Authors' contributions: XYZ, TLH and JQL designed and performed the experiments. JJS analyzed the data. XYZ, TLH and JQL wrote and revised the article. All authors read, revised,

and approved the final manuscript.

Acknowledgements: This work was supported by National Natural Science Foundation of China, 81974331.

References

1. Ahuja CS, Wilson JR, Nori S, et al. Traumatic spinal cord injury. *Nat Rev Dis Primers* 2017; **3**: 17018.

2. Hoeffel G, Ginhoux F. Ontogeny of Tissue-Resident Macrophages. *Front Immunol* 2015; **6**: 486.

3. Gensel JC, Zhang B. Macrophage activation and its role in repair and pathology after spinal cord injury. *Brain Res* 2015; **1619**: 1-11.

4. Wang J, Chen J, Jin H, et al. BRD4 inhibition attenuates inflammatory response in microglia and facilitates recovery after spinal cord injury in rats. *J Cell Mol Med* 2019; **23**(5): 3214-23.

5. Han D, Yu Z, Liu W, et al. Plasma Hemopexin ameliorates murine spinal cord injury by switching microglia from the M1 state to the M2 state. *Cell Death Dis* 2018; **9**(2): 181.

6. Wang C, Wang Q, Lou Y, et al. Salidroside attenuates neuroinflammation and improves functional recovery after spinal cord injury through microglia polarization regulation. *Journal of cellular and molecular medicine* 2018; **22**(2): 1148-66.

7. Gaojian T, Dingfei Q, Linwei L, et al. Parthenolide promotes the repair of spinal cord injury by modulating M1/M2 polarization via the NF-κB and STAT 1/3 signaling pathway. *Cell death discovery* 2020; **6**: 97.

8. Zhou J, Li Z, Wu T, Zhao Q, Zhao Q, Cao Y. LncGBP9/miR-34a axis drives macrophages toward a phenotype conducive for spinal cord injury repair via STAT1/STAT6 and SOCS3. *J Neuroinflammation* 2020; **17**(1): 134.

9. Li L, Ni L, Heary RF, Elkabes S. Astroglial TLR9 antagonism promotes chemotaxis and alternative activation of macrophages via modulation of astrocyte-derived signals: implications for spinal cord injury. *J Neuroinflammation* 2020; **17**(1): 73.

10. Kong FQ, Zhao SJ, Sun P, et al. Macrophage MSR1 promotes the formation of foamy macrophage and neuronal apoptosis after spinal cord injury. *J Neuroinflammation* 2020; **17**(1): 62.

11. Van den Bossche J, O'Neill LA, Menon D. Macrophage Immunometabolism: Where Are We (Going)? *Trends Immunol* 2017; **38**(6): 395-406.

12. Rodriguez-Cuenca S, Cocheme HM, Logan A, et al. Consequences of long-term oral administration of the mitochondria-targeted antioxidant MitoQ to wild-type mice. *Free Radic Biol Med* 2010; **48**(1): 161-72.

13. McManus M, Murphy M, Franklin J. The mitochondria-targeted antioxidant MitoQ prevents loss of spatial memory retention and early neuropathology in a transgenic mouse model of Alzheimer's disease. *The Journal of neuroscience : the official journal of the Society for Neuroscience* 2011; **31**(44): 15703-15.

14. Chen W, Guo C, Jia Z, et al. Inhibition of Mitochondrial ROS by MitoQ Alleviates White Matter Injury and Improves Outcomes after Intracerebral Haemorrhage in Mice. *Oxidative medicine and cellular longevity* 2020; **2020**: 8285065.

15. Chen X, Wang L, Song X. Mitoquinone alleviates vincristine-induced neuropathic pain through inhibiting oxidative stress and apoptosis via the improvement of mitochondrial dysfunction. *Biomedicine & pharmacotherapy = Biomedecine & pharmacotherapie* 2020; **125**: 110003.

16. Jiang W, Li M, He F, Zhou S, Zhu L. Targeting the NLRP3 inflammasome to attenuate spinal cord injury in mice. *J Neuroinflammation* 2017; **14**(1): 207.

17. Fischer AH, Jacobson KA, Rose J, Zeller R. Hematoxylin and eosin staining of tissue and cell sections. *CSH Protoc* 2008; **2008**: pdb.prot4986.

18. Carriel V, Campos A, Alaminos M, Raimondo S, Geuna S. Staining Methods for Normal and Regenerative Myelin in the Nervous System. *Methods Mol Biol* 2017; **1560**: 207-18.

19. Borjini N, Sivilia S, Giuliani A, et al. Potential biomarkers for neuroinflammation and neurodegeneration at short and long term after neonatal hypoxic-ischemic insult in rat. *J Neuroinflammation* 2019; **16**(1): 194.

20. Vannella KM, Wynn TA. Mechanisms of Organ Injury and Repair by Macrophages. *Annu Rev Physiol* 2017; **79**: 593-617.

21. Kwiecien J, Dabrowski W, Dąbrowska-Bouta B, et al. Prolonged inflammation leads to ongoing damage after spinal cord injury. *PloS one* 2020; **15**(3): e0226584.

22. Duan H, Wu Q, Yao X, et al. Nafamostat mesilate attenuates inflammation and apoptosis and promotes locomotor recovery after spinal cord injury. *CNS neuroscience & therapeutics* 2018; **24**(5): 429-38.

23. Xia P, Gao X, Duan L, Zhang W, Sun Y. Mulberrin (Mul) reduces spinal cord injury (SCI)-induced apoptosis, inflammation and oxidative stress in rats via miroRNA-337 by targeting Nrf-2. *Biomedicine & pharmacotherapy = Biomedecine & pharmacotherapie* 2018; **107**: 1480-7.

24. Kumar H, Jo M, Choi H, et al. Matrix Metalloproteinase-8 Inhibition Prevents Disruption of Blood-Spinal Cord Barrier and Attenuates Inflammation in Rat Model of Spinal Cord Injury. *Molecular neurobiology* 2018; **55**(3): 2577-90.

25. Li D, Tian H, Li X, et al. Zinc promotes functional recovery after spinal cord injury by activating Nrf2/HO-1 defense pathway and inhibiting inflammation of NLRP3 in nerve cells. *Life sciences* 2020; **245**: 117351.

26. Torres-Espín A, Forero J, Fenrich K, et al. Eliciting inflammation enables successful rehabilitative training in chronic spinal cord injury. *Brain : a journal of neurology* 2018; **141**(7): 1946-62.

27. Chen S, Ye J, Chen X, et al. Valproic acid attenuates traumatic spinal cord injury-induced inflammation via STAT1 and NF-κB pathway dependent of HDAC3. *J Neuroinflammation* 2018; **15**(1): 150.

28. Yuan Y, Chen Y, Peng T, et al. Mitochondrial ROS-induced lysosomal dysfunction impairs autophagic flux and contributes to M1 macrophage polarization in a diabetic condition. *Clin Sci (Lond)* 2019; **133**(15): 1759-77.

29. Fuhrmann DC, Brune B. Mitochondrial composition and function under the control of hypoxia. *Redox Biol* 2017; **12**: 208-15.

30. Yao Q, Khan MP, Merceron C, et al. Suppressing Mitochondrial Respiration Is Critical for Hypoxia Tolerance in the Fetal Growth Plate. *Dev Cell* 2019; **49**(5): 748-63 e7.

31. Feng J, Li L, Ou Z, et al. IL-25 stimulates M2 macrophage polarization and thereby promotes mitochondrial respiratory capacity and lipolysis in adipose tissues against obesity. *Cellular & molecular immunology* 2018; **15**(5): 493-505.

32. Li C, Ding X, Xiang D, et al. Enhanced M1 and Impaired M2 Macrophage Polarization and Reduced Mitochondrial Biogenesis via Inhibition of AMP Kinase in Chronic Kidney Disease. *Cellular physiology and biochemistry : international journal of experimental cellular physiology, biochemistry, and pharmacology* 2015; **36**(1): 358-72.

33. Tan Z, Xie N, Cui H, et al. Pyruvate dehydrogenase kinase 1 participates in macrophage polarization via regulating glucose metabolism. *Journal of immunology (Baltimore, Md : 1950)* 2015; **194**(12): 6082-9.

34. Lu H, Wu L, Liu L, et al. Quercetin ameliorates kidney injury and fibrosis by modulating M1/M2 macrophage polarization. *Biochem Pharmacol* 2018; **154**: 203-12.

35. Du R, Sun H, Hu Z, Lu M, Ding J, Hu G. Kir6.1/K-ATP channel modulates microglia phenotypes: implication in Parkinson's disease. *Cell death & disease* 2018; **9**(3): 404.

36. Van den Bossche J, Lamers WH, Koehler ES, et al. Pivotal Advance: Arginase-1-independent polyamine production stimulates the expression of IL-4-induced alternatively activated macrophage markers while inhibiting LPS-induced expression of inflammatory genes. *J Leukoc Biol* 2012; **91**(5): 685-99.

37. Jha AK, Huang SC, Sergushichev A, et al. Network integration of parallel metabolic and transcriptional data reveals metabolic modules that regulate macrophage polarization. *Immunity* 2015; **42**(3): 419-30.

38. Bock FJ, Tait SWG. Mitochondria as multifaceted regulators of cell death. *Nat Rev Mol Cell Biol* 2020; **21**(2): 85-100.

39. Wei Y, Zhang YJ, Cai Y, Xu MH. The role of mitochondria in mTOR-regulated longevity. *Biol Rev Camb Philos Soc* 2015; **90**(1): 167-81.

40. Morita M, Prudent J, Basu K, et al. mTOR Controls Mitochondrial Dynamics and Cell Survival via MTFP1. *Mol Cell* 2017; **67**(6): 922-35 e5.

41. Laforge M, Rodrigues V, Silvestre R, et al. NF-κB pathway controls mitochondrial dynamics. *Cell Death Differ* 2016; **23**(1): 89-98.

42. Zhong Z, Umemura A, Sanchez-Lopez E, et al. NF-κB Restricts Inflammasome Activation via Elimination of Damaged Mitochondria. *Cell* 2016; **164**(5): 896-910.

Figures

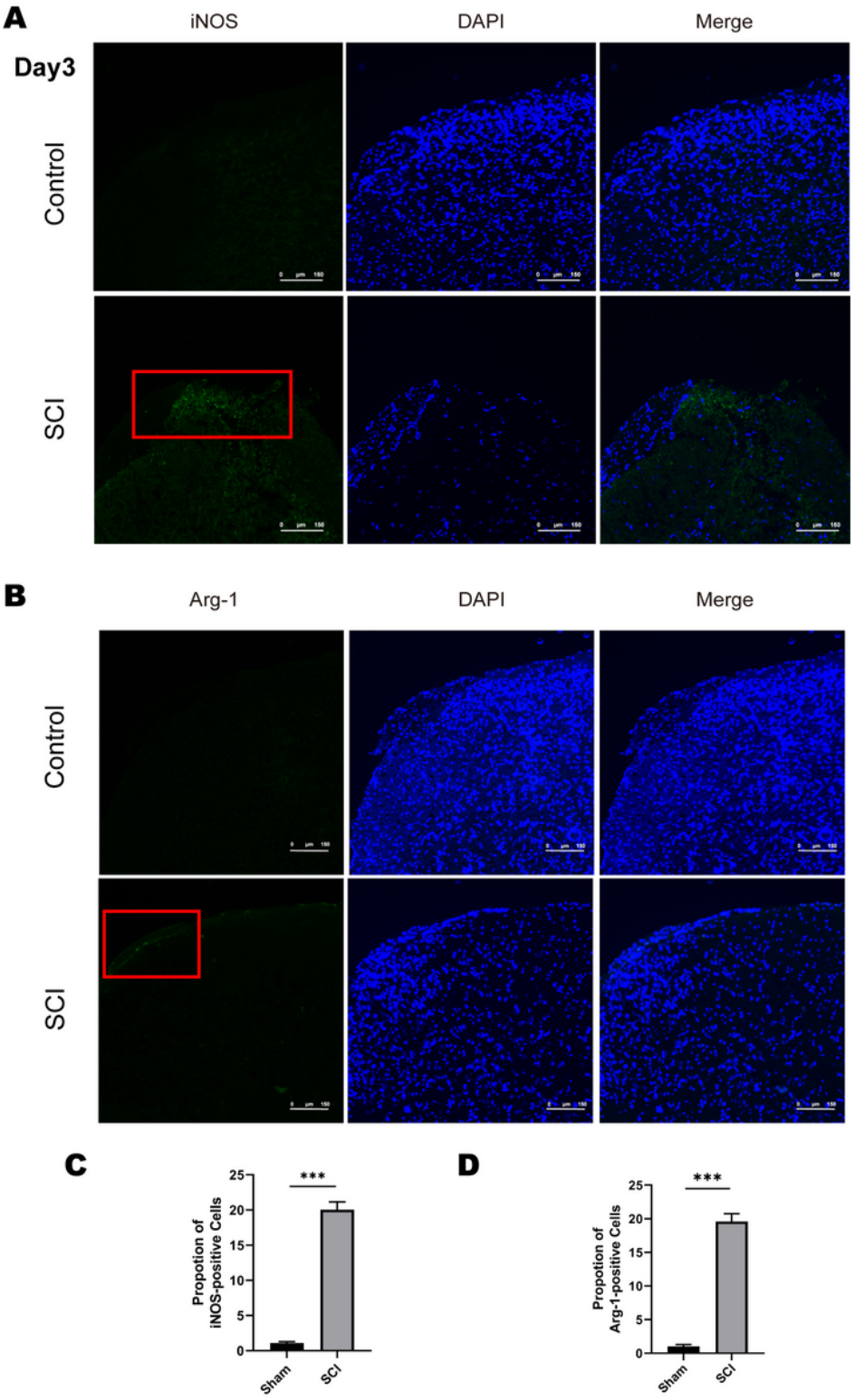

Figure 1

The natural expression of M1-polarized and M2-polarizaed macrophage/microglia after SCI on day 3. (A) Immunofluorescence label of iNOS-positive cells for M1-like polarization of macrophage/microglia in the Sham (control) and SCI groups (n=3). (B) Immunofluorescence label of Arg-1-positive cells for M2-like polarization of macrophage/microglia in the Sham (control) and SCI groups (n=3). (C-D) Quantitative analysis of the results in panels. (n =3, nsno significant difference, *p□0.05, **p□0.01, ***p < 0.001, ****p□ 0.0001).

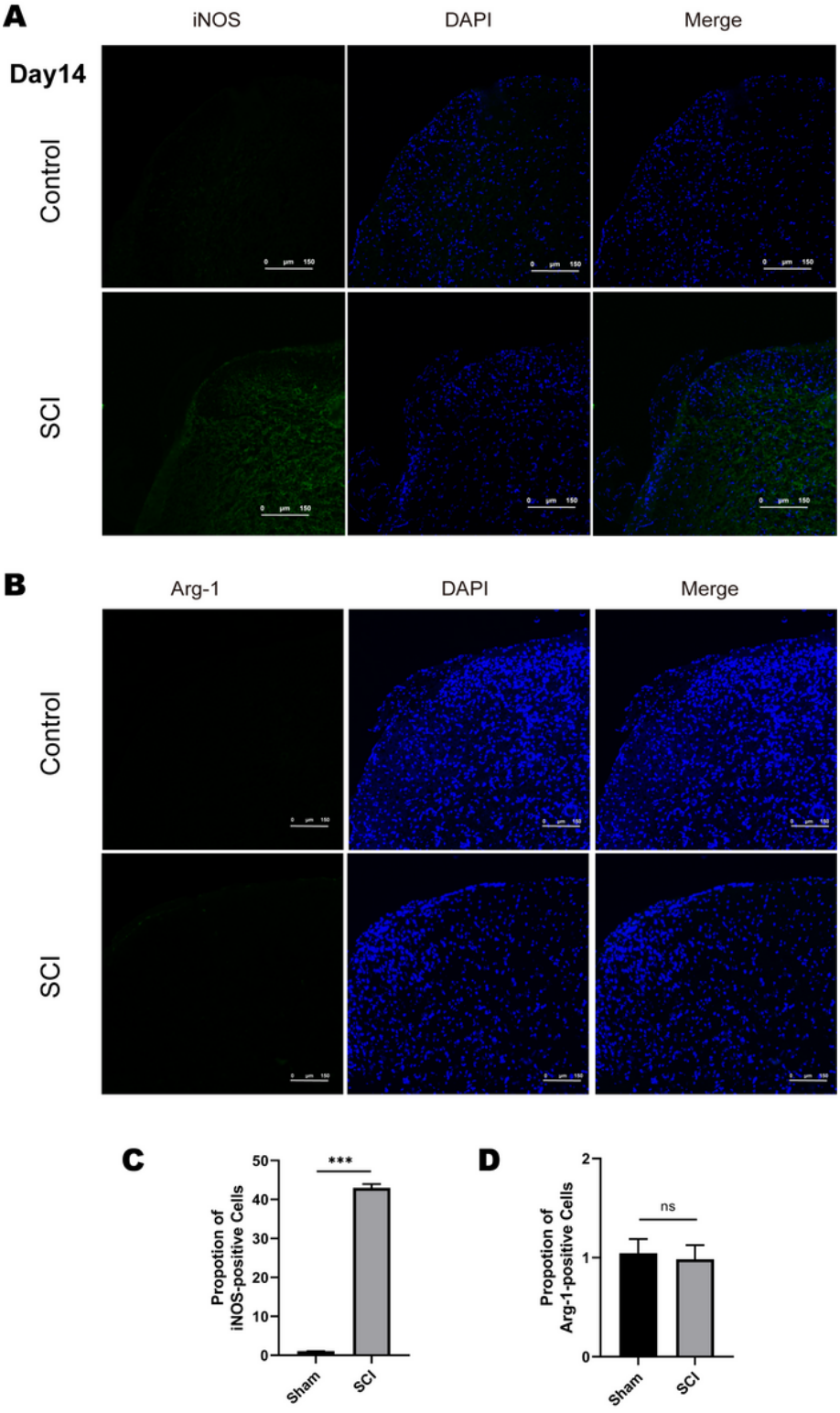

Figure 2

The natural expression of M1-polarized and M2-polarizaed macrophage/microglia after SCI on day 14. (A) Immunofluorescence label of iNOS-positive cells for M1-like polarization of macrophage/microglia in the Sham (control) and SCI groups (n=3). (B) Immunofluorescence label of Arg-1-positive cells for M2-like polarization of macrophage/microglia in the Sham (control) and SCI groups (n=3). (C-D) Quantitative analysis of the results in panels. (n =3, nsno significant difference, *p□0.05, **p□0.01, ***p < 0.001, ****p□ 0.0001).

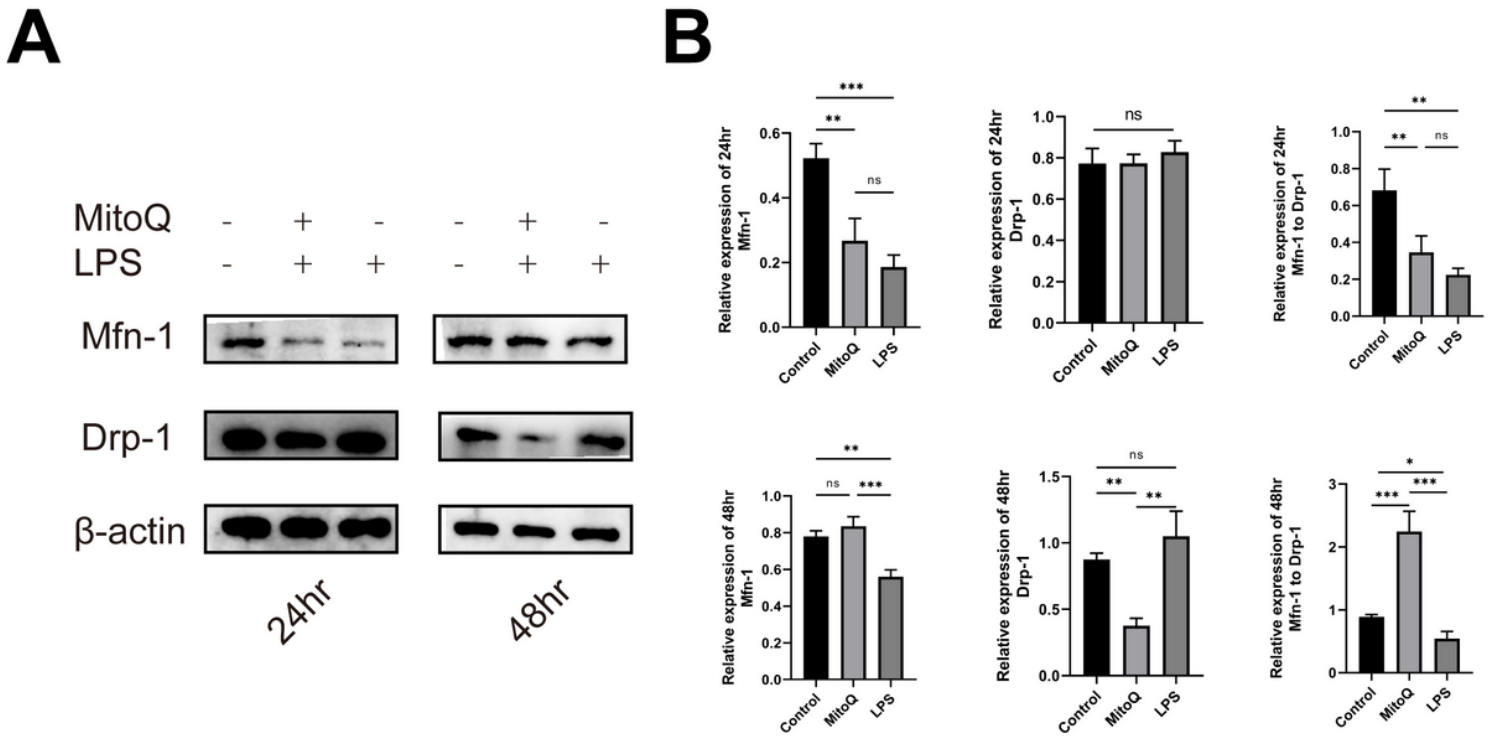

Figure 3

MitoQ attenuates LPS-induced mitochondrial biodynamic in BV2 cells. (A) Expression of mitochondrial-fusion related protein Mfn-1/2 and mitochondrial-fission related protein Drp-1 after 24hr and 48hr treatment among control, MitoQ (12hr pretreating with MitoQ :200nM and combined treatment MitoQ:200nM and LPS:100ng/ml) and LPS (100ng/ml) groups. (B) Quantification analysis of expression of Mfn-1 and Drp-1 and the ratio of Mfn-1/Drp-1 in panel A. (n =3, nsno significant difference, *p□0.05, **p □0.01, ***p < 0.001, ****p□0.0001).

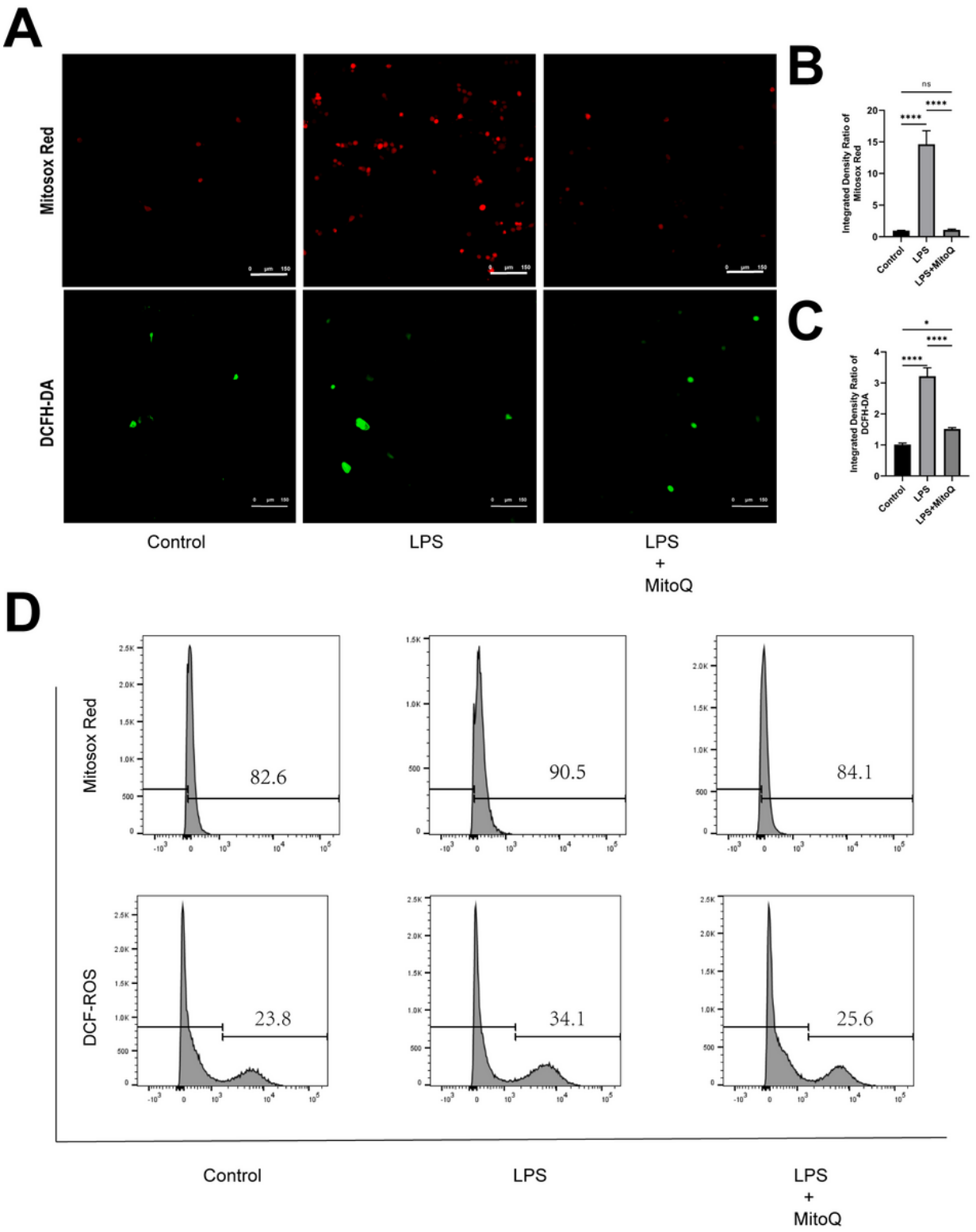

Figure 4

MitoQ attenuates LPS-induced oxidative stress in BV2 cells. (A) Evaluation of mitochondrial-specific ROS and cellular ROS through the label of Mitosox Red and DCFH-DA staining in BV2 cells among control, LPS and MitoQ groups. (B-C) Quantification of fluorescence intensity in panel A. (D) Flow cytometry assay of Mitosox Red and DCFH-DA fluorescence intensity. (n =3, nsno significant difference, *p□0.05, **p□0.01, ***p < 0.001, ****p□0.0001).

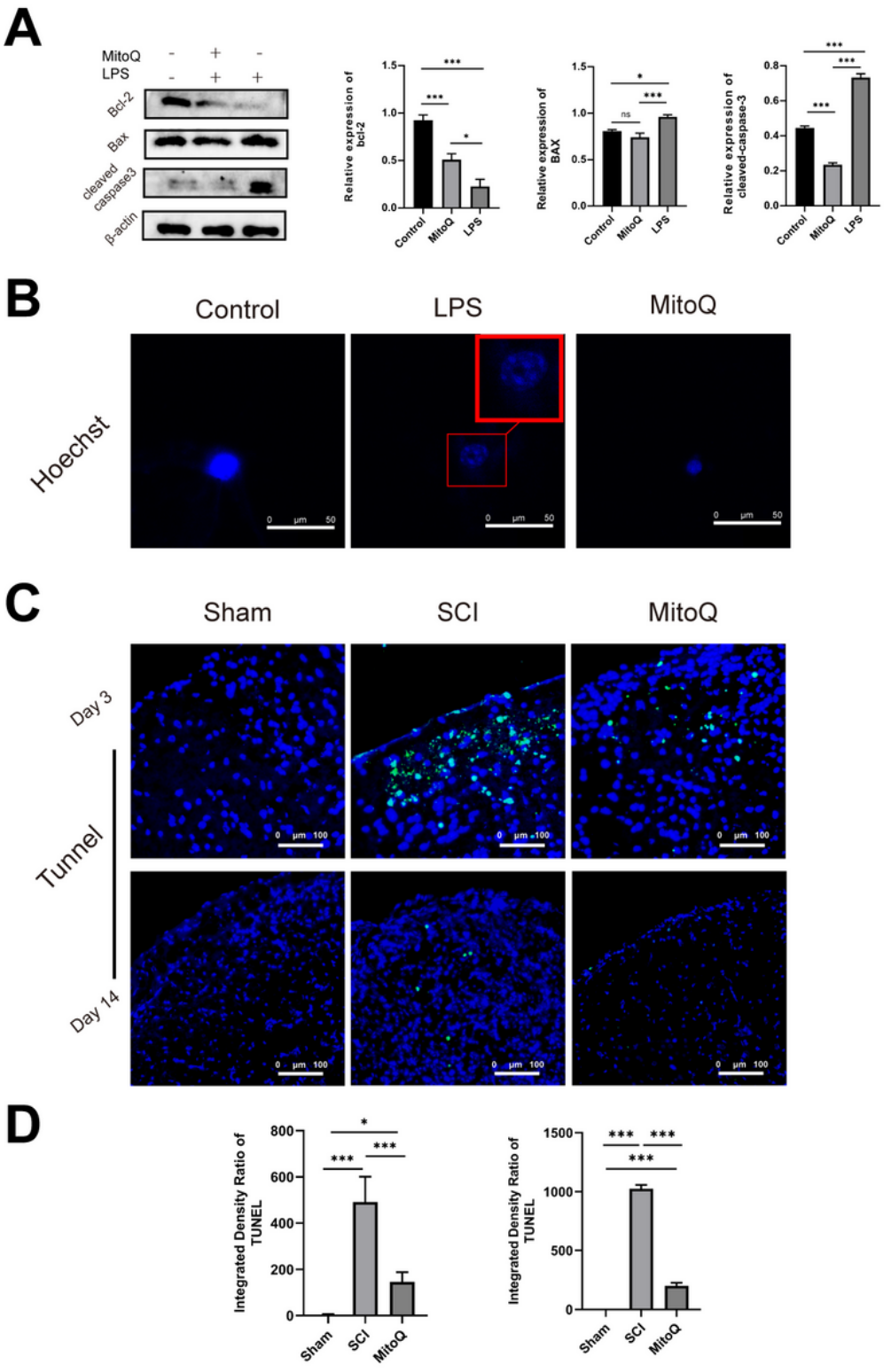

Figure 5

MitoQ inhibits cell apoptosis in SCI animal models and LPS-challenging BV2 cells. (A) Expression and quantification of cellular apoptosis related protein Bax, Bcl-2 and cleaved caspase 3 among control, LPS and MitoQ groups. (B) Hochest staining for cell nucleus visualization among Control, LPS and MitoQ groups. (C) Tunel staining of lesion site on day 3 and day 14 after SCI. (D) Quantification of Tunel

staining positive expression ratio to Control group. (n =3, nsno significant difference, *p0.05, **p0.01, ***p < 0.001, ****p0.0001).

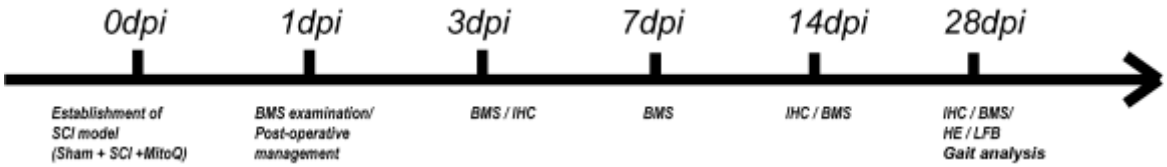

Figure 6

Timeline of in-vivo examination.

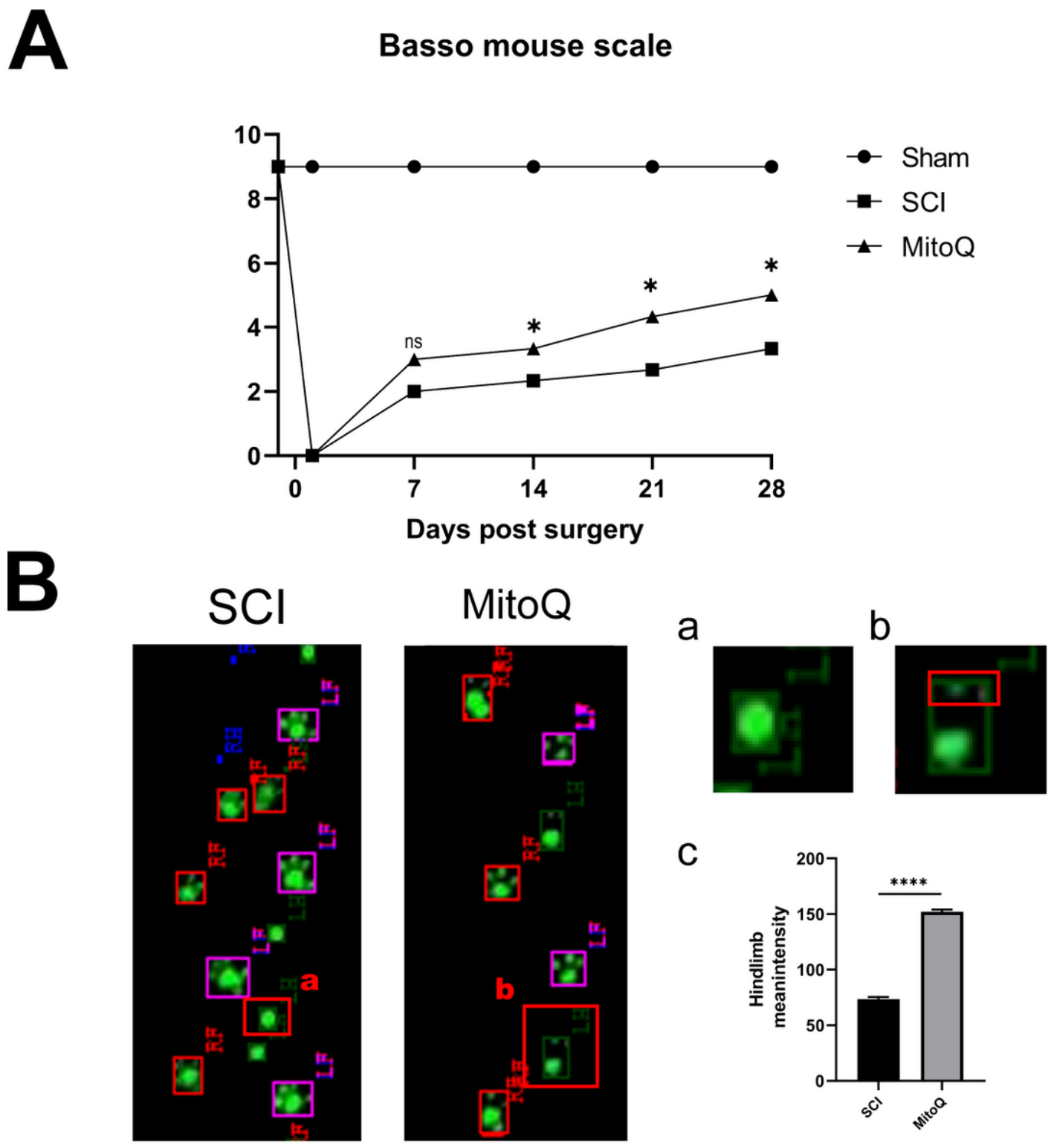

Figure 7

MitoQ treatment promotes function recovery of hindlimb locomotion and walking gait. (A) Open field Basso Mouse Scale (BMS) locomotor examination performed weekly among Sham, SCI and MitoQ groups. (B) Cat walk analysis for gait assay between SCI and MitoQ groups. (a-b) Zoomed up hindlimb print of SCI and MitoQ groups. (C) Quantification analysis of hindlimb intensity between SCI and MitoQ groups. (n =3, nsno significant difference, *p□0.05, **p□0.01, ***p < 0.001, ****p□0.0001).

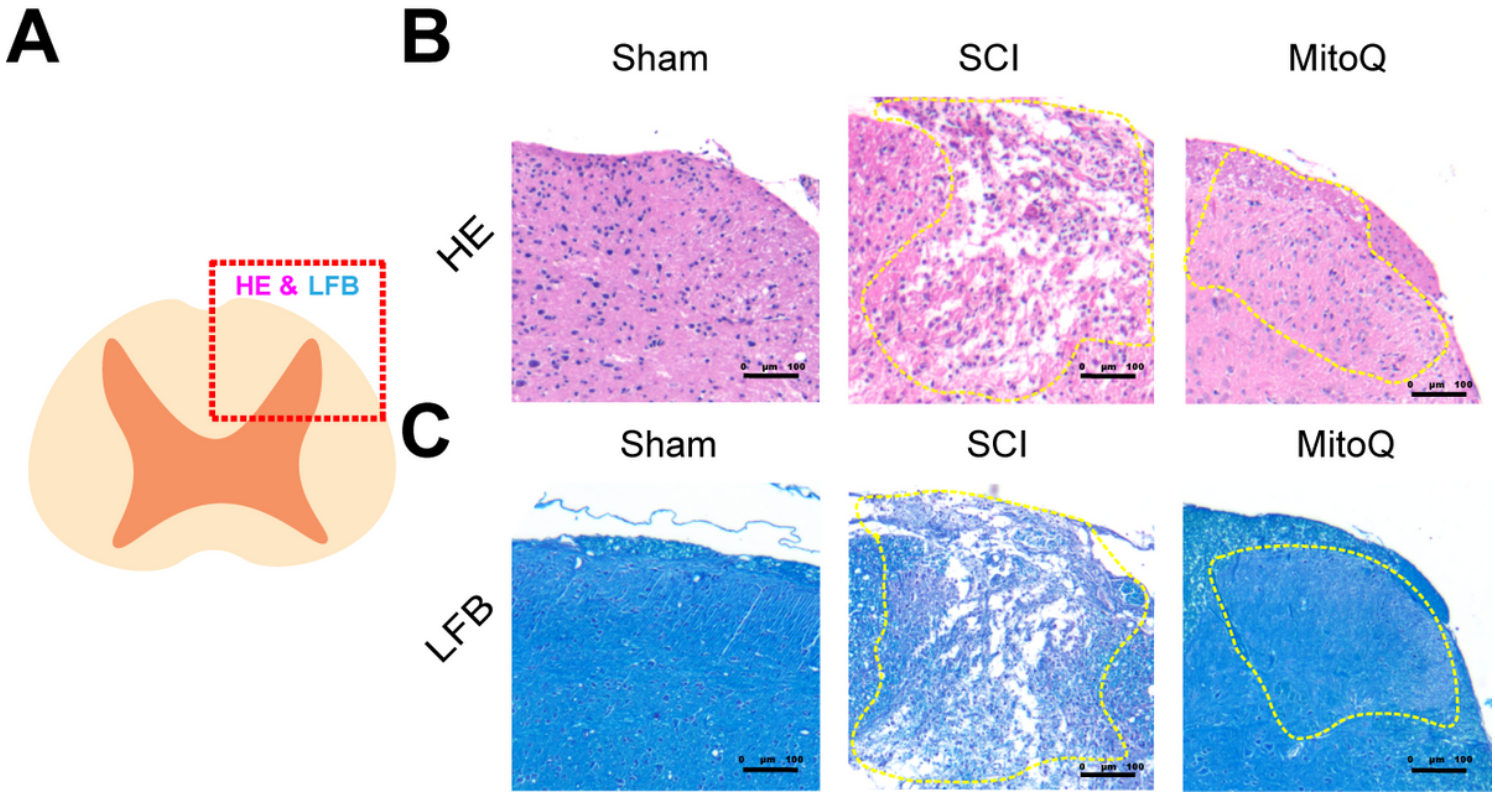

Figure 8

MitoQ promotes tissue and neural preservation after SCI. (A) Mimic diagram of position of clip-compression and HE/LFB examination. (B) Hematoxylin-eosin (HE) staining for identify the tissue preservation among Sham, SCI and MitoQ groups. (C) Luxol Fast Blue (LFB) staining to identify the myeline loss among Sham, SCI and MitoQ groups. (n=3)

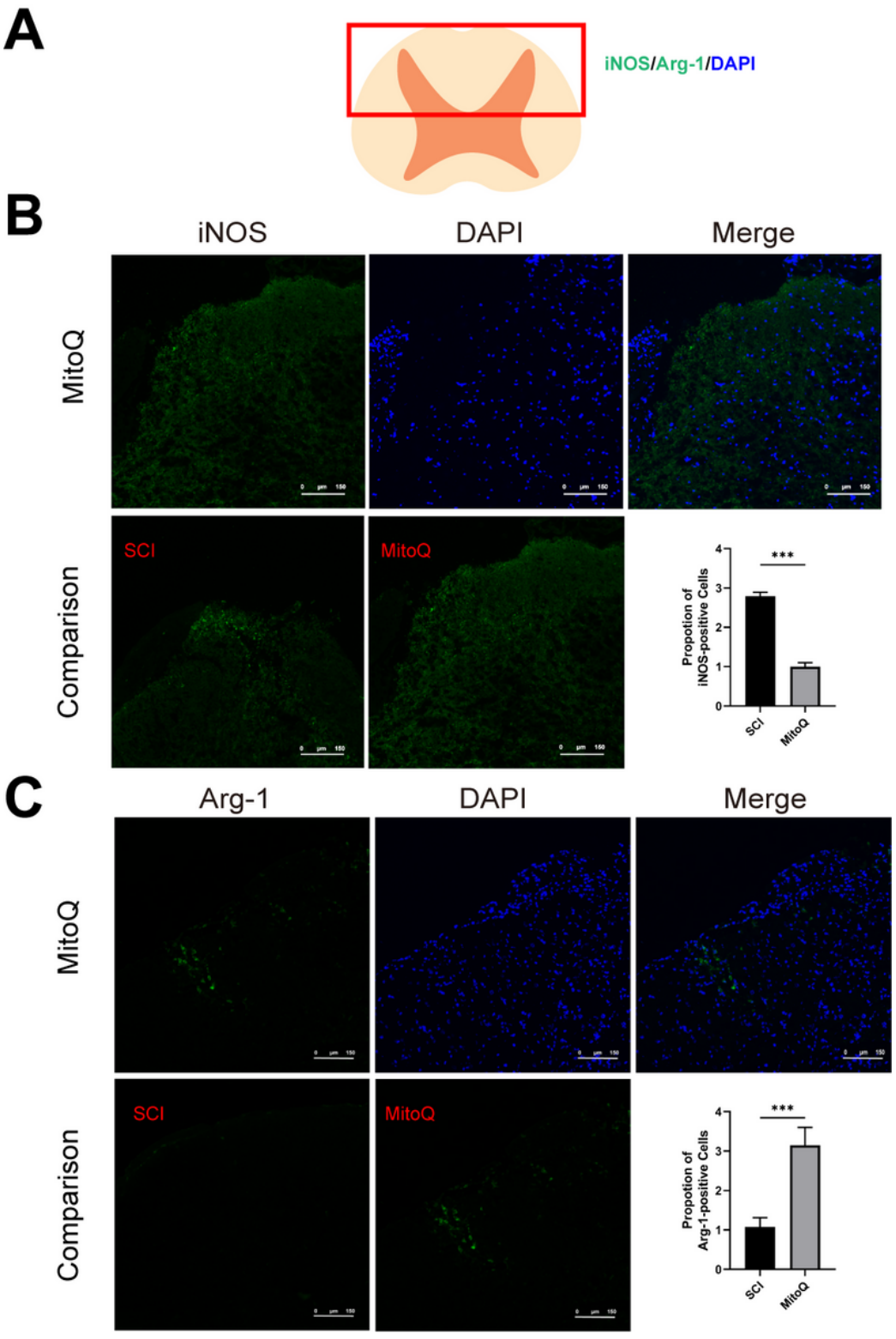

Figure 9

MitoQ promotes M2-like polarization and inhibits M1-like polarization after SCI on day 3. Figure of SCI group from Figure 1. (A) Diagrammatic sketch of lesion site and immunofluorescence staining. (B) Immunofluorescence staining and quantification analysis of iNOS in lesion site. (C) Immunofluorescence staining and quantification analysis of Arg-1 in lesion site. (n =3, nsno significant difference, *p□0.05, **p□ 0.01, ***p < 0.001, ****p□0.0001).

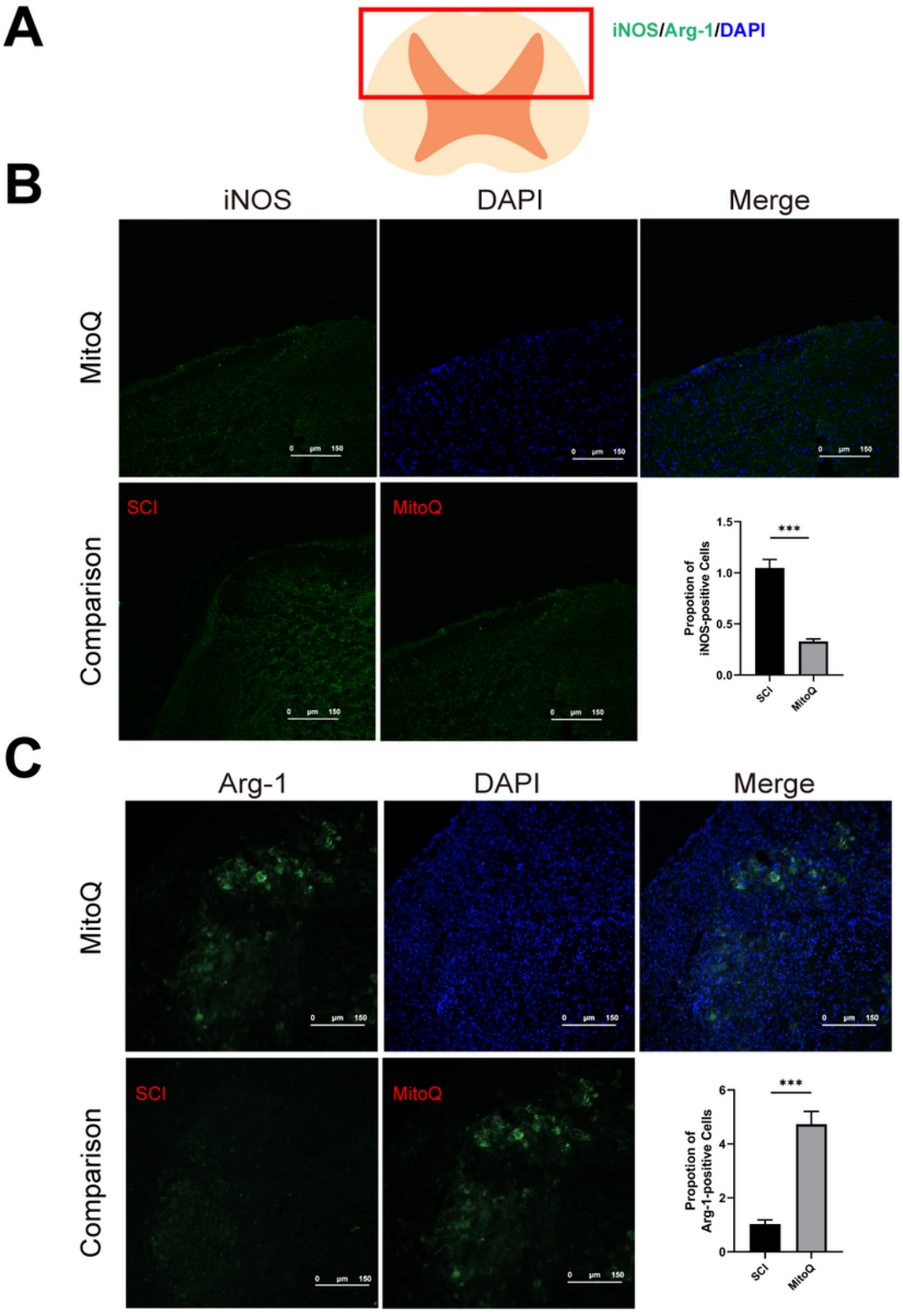

Figure 10

MitoQ promotes M2-like polarization and inhibits M1-like polarization after SCI on day 14. Figure of SCI group from Figure 2 (A) Diagrammatic sketch of lesion site and immunofluorescence staining. (B) Immunofluorescence staining and quantification analysis of iNOS in lesion site. (C) Immunofluorescence staining and quantification analysis of Arg-1 in lesion site. (n =3, nsno significant difference, *p□0.05, **p□ 0.01, ***p < 0.001, ****p□0.0001).

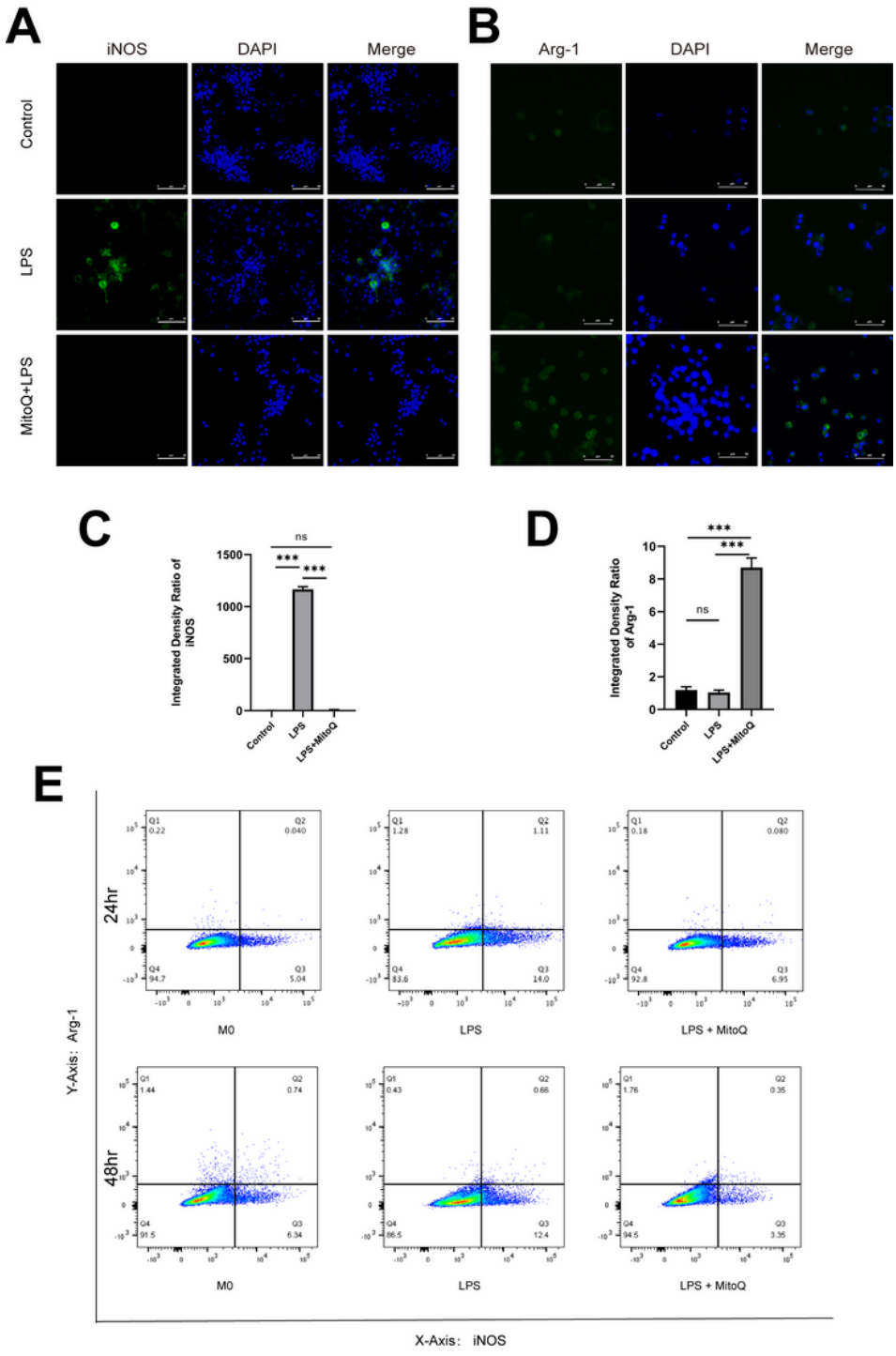

Figure 11

MitoQ promotes M2-like polarization and inhibits M1-like polarization in BV2 cells. (A) Immunofluorescence staining of iNOS in BV2 cells among control, LPS and MitoQ + LPS groups. (B) Immunofluorescence staining of Arg-1 in BV2 cells among control, LPS and MitoQ + LPS groups. (C-D) Quantification of immunofluorescence staining in panel A and B. (E) Flow cytometry result of treated BV2

cells among control, LPS and MitoQ + LPS groups after 24 and 48 h treatment (X-axis: iNOS, Y-axis: Arg-1). (n =3, nsno significant difference, *p0.05, **p0.01, ***p < 0.001, ****p0.0001).

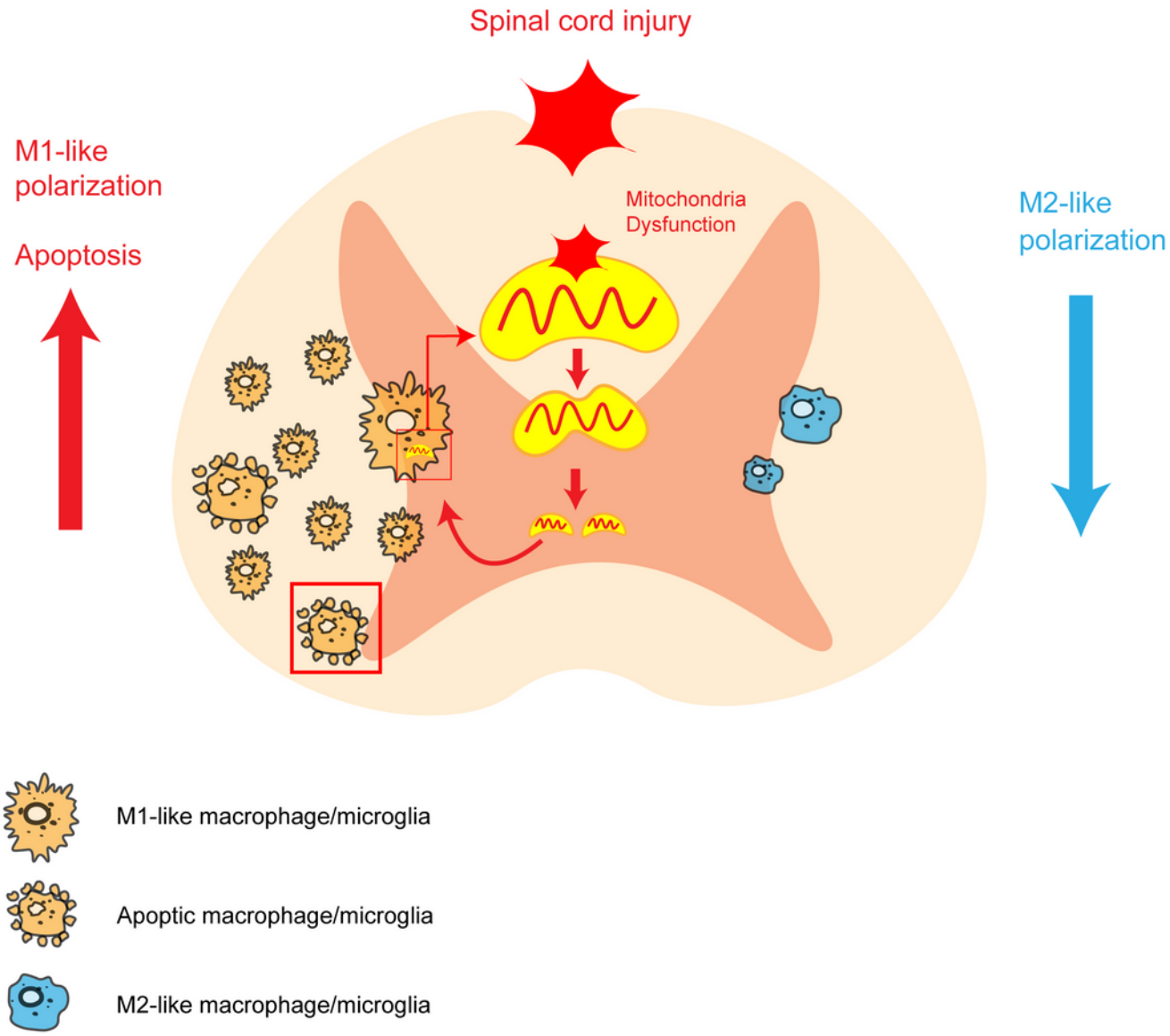

Figure 12

Graphic mechanism.